

New dimensions in acidocalcisome research: the potential of cryo-EM to uncover novel aspects of protozoan parasite physiology

Ingrid Augusto,^{1,2} Moara Lemos,^{1,3} Wendell Girard-Dias,^{1,4} José de Anchieta Oliveira Filho,⁵ Pedro G. Pascutti,⁵ Wanderley de Souza,^{1,2,6} Kildare Miranda^{1,2,6}

AUTHOR AFFILIATIONS See affiliation list on p. 12.

ABSTRACT Cryo-electron microscopy (cryo-EM) has revolutionized structural biology by enabling high-resolution, near-native visualization of macromolecular structures and entire cells. Its application to etiologic agents of diseases is an expanding field, particularly for those caused by viruses or unicellular eukaryotes, such as protozoan parasites and fungi. This review focuses on acidocalcisomes—ion-rich, multifunctional organelles essential for cell physiology and survival in several pathogens. The structure and function of these organelles are examined through a range of electron microscopy techniques, using *Trypanosoma cruzi* as a model. The advantages and limitations of the methods employed to study acidocalcisome morphofunctional organization—such as chemical fixation, plunge and high-pressure freezing, cryo-electron microscopy of vitrified sections (CEMOVIS), freeze-drying, freeze substitution, tomography, and microanalysis using X rays and inelastic scattered electrons—are discussed, alongside their contributions to our current understanding of acidocalcisome structure and function. Recent advances in cryo-EM and its potential to address longstanding questions and fill existing gaps in our understanding of parasite ion mobilization mechanisms and physiology are also discussed.

KEYWORDS *Trypanosoma cruzi*, acidocalcisomes, ion nanodomains, biomolecular condensates, cryo electron microscopy

Cryo-electron microscopy (cryo-EM) is widely regarded as one of the most transformative innovations in structural biology, revolutionizing the field by enabling the determination of macromolecular structures at near-atomic resolution with unprecedented speed. The detailed structural models generated through cryo-EM have provided invaluable insights into macromolecular function and their roles in biological processes (1). Recognized in 2017 with the Nobel Prize in Chemistry awarded to its developers, cryo-EM has made remarkable progress in recent years, particularly in achieving high-resolution *in situ* studies of whole cells across diverse biological systems (2–5). A compelling example of the impact of cryo-EM in microbiology was its contribution to the development of COVID-19 vaccines, as well as in diagnostics and monitoring immune responses to vaccination (6–9). Notably, cryo-EM remains the only methodology capable of conducting *in situ* analyses in a state closely resembling the native *in vivo* environment, producing highly reliable and biologically relevant results. Nevertheless, despite its significant advancements across various fields of microbiology (10), the application of cryo-EM to studying neglected diseases caused by protozoan parasites remains in its early stages (11, 12).

Editor Marcio Rodrigues, Instituto Carlos Chagas, Curitiba, Brazil

Address correspondence to Kildare Miranda, kmiranda@biof.ufrj.br, or Ingrid Augusto, ingrid.augusto@biof.ufrj.br.

The authors declare no conflict of interest.

Published 8 April 2025

Copyright © 2025 Augusto et al. This is an open-access article distributed under the terms of the [Creative Commons Attribution 4.0 International license](https://creativecommons.org/licenses/by/4.0/).

CHALLENGES IN APPLYING CRYO-EM TO PROTOZOAN PARASITE RESEARCH

Cryo-electron tomography (cryo-ET) has been applied to a wide range of microorganisms, including protozoan parasites. Like room-temperature EM techniques, one of the main limitations of cryo-ET is the sample thickness, which to some extent restricts high-resolution visualization of thicker regions. As a result, most *in situ* cryo-EM studies have focused on parasites from the phylum Apicomplexa, such as *Plasmodium*, *Toxoplasma*, and *Cryptosporidium*. These studies, likely facilitated by the small size of these organisms, have predominantly investigated the cell invasion machinery in isolated parasites. Works involving infective stages interacting with host cells have only recently emerged (11, 13–21). In contrast, the use of cryo-EM for *in situ* studies of whole cells in larger organisms, such as *Giardia* and *Trichomonas*, remains rare. Experiments in these organisms have primarily been limited to the analysis of isolated proteins or structures within membrane-extracted cells (22–27).

In pathogenic trypanosomatids, various approaches have been employed to address the limitations posed by cell thickness. These include the use of anucleated *Trypanosoma brucei* mutants (28), combining cryo-EM with STEM mode (29, 30), and producing cryosections via cryoultramicrotomy or lamellae through milling with a focused ion beam microscope (Cryo-FIB SEM) (31–33). Despite these advances, most studies have primarily focused on thinner cellular regions, particularly the flagellum of *T. brucei* (32, 34–36). However, the structure of thicker regions and, more importantly, the physiological processes occurring in these areas remain largely unexplored.

In this review, we revisited the contributions of electron microscopy (EM) methods to parasite research, with a particular emphasis on acidocalcisomes, multifunctional organelles that play essential physiological roles in a wide variety of cells. Additionally, we explore how cryo-EM can uncover new aspects of protozoan biology, broadening our current understanding of their structure, function, and physiology.

THE ACIDOCALCISOMES

Acidocalcisomes are organelles ranging between 100 and 600 nm in diameter, characterized by an acidic, electron-dense matrix composed of phosphate polymers (polyphosphates [PolyP]) bound to ions. They were initially described in various organisms, including bacteria, plants, and protists—such as trypanosomatids—where they were originally referred to as volutine granules (37–41). Later, this organelle was identified in yeast, where they were termed “polyphosphate bodies” due to the presence of polyphosphate chains (37, 42, 43). The definitive naming of acidocalcisomes came after the identification of proton and calcium pumps on their surface in *T. brucei* and *T. cruzi* (43–45). Acidocalcisomes have since been observed in other trypanosomatids (*Leishmania* spp., *Leptomonas* spp., *Phytomonas*, and various monogenetic parasites), as well as in diverse groups, such as Apicomplexa (*Toxoplasma gondii* and *Plasmodium* spp.), algae (*Chlamydomonas reinhardtii*), fungi (*Dictyostelium discoideum*), insects, echinoderms, birds, and mammals, including human platelets, indicating their evolutionary conservation (43, 46–53).

In trypanosomatids, acidocalcisome membranes contain proteins that regulate the pH and ion composition of the matrix, including proton pumps, such as the vacuolar H⁺-pyrophosphatase (V-H⁺-PPase) (54), vacuolar H⁺-ATPase (V-H⁺-ATPase), and calcium ATPase (Ca²⁺-ATPase) (45, 55). Other key components include the zinc transporter (ZnT) and the inositol 1,4,5-trisphosphate receptor (IP3-R) (56–60). Additionally, a polyphosphate kinase (VTC) (61, 62), involved in PolyP synthesis and translocation, and the water channel aquaporin 1 (AQP1) (63) have also been identified on the membrane of acidocalcisomes.

Acidocalcisomes play crucial roles in osmoregulation, pH control, cellular homeostasis, calcium signaling, and cell bioenergetics (64). In trypanosomatids, the pH of acidocalcisomes adjusts in response to H⁺ concentrations in the cytoplasm, mitochondrial matrix, and other acidic compartments, including the acidocalcisomes themselves

(65). A decrease in the activity of the proton pumps within acidocalcisomes leads to reduced organelle acidification and a corresponding drop in cytoplasmic pH (66).

Additionally, acidocalcisomes serve as the primary reservoir for intracellular Ca^{2+} . Calcium uptake and release, mediated by Ca^{2+} -ATPase and inositol 1,4,5-trisphosphate receptor (IP3-R), respectively, position this organelle as central to calcium signaling. These processes directly influence mitochondrial activity, cellular bioenergetics, and parasite infectivity (59, 67–69).

The electron-dense, acidified content of acidocalcisomes, rich in Ca^{2+} and phosphate chains (polyP), is a common feature across many organisms, although variations exist in the ion composition of the matrix. For instance, in *C. reinhardtii*, calcium, magnesium, and zinc ions have been identified in acidocalcisomes (47, 70), whereas in human platelets, only calcium and potassium ions have been found (46).

In trypanosomatids, the acidocalcisome matrix contains sodium, magnesium, potassium, calcium, iron, zinc, and phosphate polymers (53, 71–74). However, differences in the number, volume, and diameter of acidocalcisomes, as well as the concentrations of ions within their matrix, have been registered across species (73).

ACIDOCALCISOME STRUCTURE AND COMPOSITION UNVEILED THROUGH DIFFERENT EM PREPARATION AND IMAGING TECHNIQUES

Chemical fixation: advantages and limitations

Fixation is the initial and most critical step in the preparation of biological samples for electron microscopy. Its primary purpose is to halt biological activity, preserving the structural organization and three-dimensional integrity of the sample with minimal alteration (75). This can be achieved either chemically, using fixation reagents, or mechanically, through cryofixation, using various methods.

Chemical fixation fundamentally involves the immobilization of cellular components through the formation of cross-links between and within molecules (76, 77). The primary fixatives commonly used for routine electron microscopy are aldehyde-based fixatives, such as formaldehyde and glutaraldehyde, which provide enhanced preservation of cellular components when combined (78). Following aldehyde fixation, osmium tetroxide is typically used to stabilize lipids and unsaturated molecules, providing improved contrast for electron microscopy analysis (79).

Despite the mechanisms of fixative reagents in immobilizing cellular structures (80, 81), the integrity of the cell membranes can be compromised during the fixation process, allowing for the diffusion of molecules that may lead to significant artifacts. Fixation with glutaraldehyde, osmium tetroxide, or a combination of both completely abolishes the selective permeability of membranes, directly interfering with the osmotic properties of cell membranes. This disruption renders them permeable to osmolytes and leads to the loss of essential ions, such as potassium and magnesium, along with ATP (82). Additionally, fixation can cause the redistribution of proteins and lipids within the sample, stimulus of membrane vesiculation or blebs, leading to cell shrinkage or swelling (80, 82–85).

Considering the ionic and acidic nature of acidocalcisomes, studying their ultrastructure using chemical fixation presents a significant challenge. They often appear as empty vacuoles containing remnant or degraded electron-dense material when fixative reagents are applied (64, 72–74, 86). While alternative fixation solutions can mitigate these artifacts (73), subsequent steps in conventional TEM sample preparation—such as dehydration, resin embedding, and ultramicrotomy—can introduce additional structural alterations (87–89).

Energy-filtered transmission electron microscopy of whole cells

Due to the high density of their core matrix, acidocalcisomes are relatively easy to visualize *in situ* using transmission electron microscopy (TEM) without requiring prior treatment. This can be achieved by adhering cells to grids coated with a continuous layer

of carbon or formvar, blotting them with filter paper, and directly visualizing them at the TEM (72, 90). High-resolution imaging of whole cells is fundamentally limited by sample thickness, which induces chromatic aberration. Significant improvements in resolution and contrast to visualize intracellular structures in whole cells can be achieved with the use of an energy-filtering TEM, which allows for the selection of electrons within specific energy loss ranges (contrast tuning), reducing chromatic aberration (72–74) (Fig. 1A).

Understanding acidocalcisome structure through cryofixation techniques

Cryofixation has been widely applied in the study of acidocalcisomes, with minor methodological variations tailored to specific objectives, whether ultrastructural, elemental analysis, or both. Each approach has significantly contributed to our understanding of this organelle; however, they also present certain limitations. Addressing both the advantages and limitations of these methods may provide valuable insights to guide future advancements in the field.

The principle of any cryofixation technique is the freezing of intracellular water from a liquid to a solid state at rapid or ultrarapid rates (around -73°C to 10^{-4} s) avoiding ice crystal formation—a process known as vitrification (92–95). This rapid immobilization of water halts physiological processes within milliseconds, eliminating the need for chemical fixatives. Consequently, cryofixation preserves cellular structures in a near-native, hydrated state, potentially achieving sub-nanometer resolution in ultrastructural analysis (96–98). Vitrification can be achieved through several methods, including the widely used plunge freezing at high velocity in atmospheric conditions or high-pressure freezing techniques, which enable vitrification of thicker samples (99, 100).

Plunge freezing involves quickly submerging a sample-carrying grid or metal support into a liquid cryogen, which has been pre-cooled with liquid nitrogen. This technique, pioneered by Dubochet et al. in the 1980s (92, 93, 101), can be performed using manual plungers or modern semi-automated systems. Commonly used alkanes include freon, propane, or ethane due to their high thermal conductivity and boiling points, ensuring rapid heat extraction (102–104). Additionally, variables, such as ambient humidity and blotting parameters used during plunging, are essential for effective vitrification (94, 103).

High-pressure freezing (HPF) is a technique that applies approximately 2,100 bar of pressure, allowing samples to reach liquid nitrogen temperatures ($\sim -196^{\circ}\text{C}$) within about 20 ms (99). The high pressure also prevents water expansion, which reduces ice nucleation and slows crystal growth, optimizing vitrification and preserving cellular structures without ice crystal formation (99, 100, 105, 106). Due to the low thermal conductivity of water, which limits heat transfer from the sample surface to its center, HPF is suitable for specimens up to 600 μm thick, including eukaryotic cells, tissues, organoids, and even whole organisms (99, 100, 104).

Once a biological sample is cryofixed, it undergoes TEM analyses. Most eukaryotic cells must be thinned to reach an optimal thickness to achieve a high signal-to-noise ratio (SNR), minimizing image blurring and ensuring the acquisition of high-resolution data (107). Among the methods used to reach deeper cell regions, conventional electron microscopy of vitreous sections (CEMOVIS) was employed for the analytical investigation of acidocalcisomes in trypanosomatids (90). In this method, a bulk vitrified sample is mounted onto a metal holder and sectioned into slices 100–200 nm thick under cryogenic conditions (108–110). Unlike ultramicrotomy performed at room temperature, these sections are typically collected on grids under dry conditions to avoid the use of floating liquids, which could alter the ultrastructure or the distribution of diffusible substances within the sample (108, 111). This method inherently introduces some artifacts due to its nature: (i) compression and cracks primarily resulting from localized stress as the sample passes through the knife edge and (ii) dry transfer of sections to the grid followed by mechanical pressure to achieve adhesion. Both steps can produce morphological deformations in the sample, which may limit the potential for high-resolution studies (111, 112).

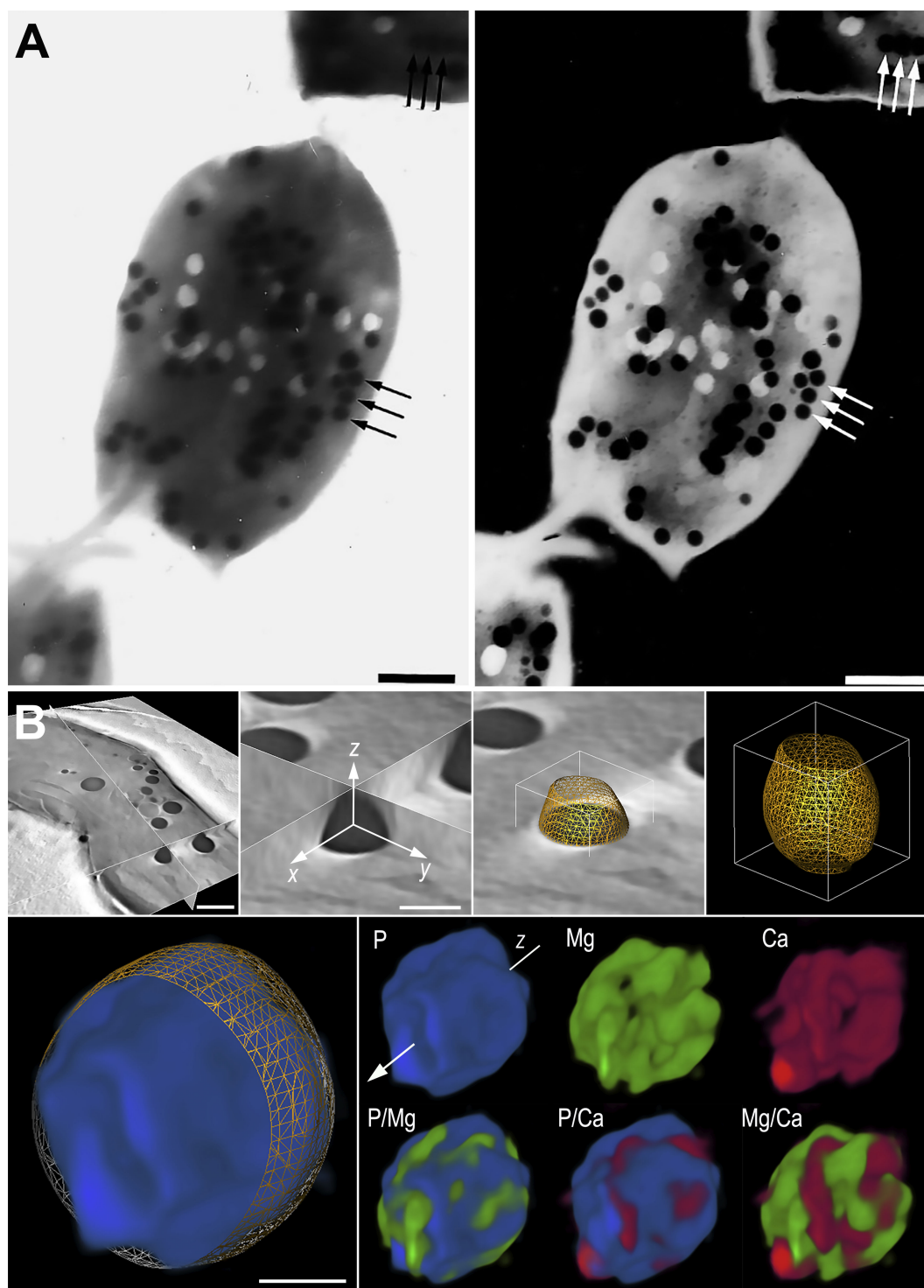


FIG 1 Visualization of acidocalcisomes in *T. cruzi* using different methodologies. (A) TEM image of an unfixed whole amastigote observed in conventional bright-field mode (left) and in electron spectroscopic imaging using contrast tuning (right), where the inelastic imaging mode provides optimal visualization of the acidocalcisomes, which are arranged in alignment (arrows). Scale bars: 700 nm. (B) Virtual section from an electron tomogram showing acidocalcisomes with 3D elemental mapping models, revealing the presence of ion nanodomains within the organelles. Scale bars = 500, 300, and 100 nm, from top left to bottom. (Panel A was reproduced from reference 72 with permission; panel B was reproduced from reference 91 with permission.)

Freeze-drying (FD) is one of the possible dehydration processes after cryofixation. It removes water from biological samples by sublimation under low temperature and

pressure, preserving structural integrity, improving stability, and enhancing contrast for electron microscopy (111, 113, 114). Freeze-dried (FD) cryosections are more stable when interacting with the electron beam, resulting in less damage and lower mass loss compared with hydrated cryosections (115). Thus, FD sections are widely used in microanalyses, such as electron energy loss spectroscopy (EELS) or energy-dispersive X-ray spectroscopy (EDS) (topics discussed in detail in the following section). In the case of hydrated sections, these are usually thicker (approximately 1 μm) to withstand the dose required for element detection without complete structural degradation (111, 115).

Despite these advantages, water extraction can alter biomolecular configurations, displace ions (particularly in compartments with high water content), and cause shrinkage of cellular structures (111, 113, 116). Additionally, the FD technique is primarily suitable for ultrastructural analyses at intermediate magnifications and has been so far insufficient for molecular structure studies that demand high resolution (111, 116).

Using CEMOVIS prior to elemental analysis, Scott et al. (90) demonstrated well-preserved epimastigote cells of *T. cruzi*, containing what they described as “spherical vacuoles of high mass density surrounded by a single membrane”—in other words, the acidocalcisomes. All observed acidocalcisomes showed a well-preserved core content with a dense matrix (90). In at least two acidocalcisomes, the membrane appeared separated from the core, a feature that could be interpreted as an artifact but allowed a clearer visualization of the membrane. Similar methodologies have continued to be applied in further analytical studies (discussed in the next section), consistently demonstrating the integrity and high density of the acidocalcisome matrix. However, the membrane and its interactions with other cytoplasmic structures were not always visible (72, 74).

An alternative methodology for dehydrating biological samples, which offers improved ultrastructural preservation, is freeze substitution (FS) following cryofixation, typically via HPF. The FS process replaces cellular water with chemical fixatives dissolved in an organic solvent at low temperatures. Samples are immersed in an FS medium, composed of ethanol, acetone, or methanol, combined with chemical fixatives that remain inactive until specific temperatures are reached (113, 117). The temperature of the sample is gradually increased to allow uniform stabilization of cellular structures throughout the entire cell volume via chemical fixation, thus reducing the likelihood of osmotic issues. This temperature progression can be automated using commercially available devices or manually controlled (113, 117, 118). After freeze substitution, samples undergo resin infiltration and embedding, as in conventional electron microscopy preparation.

Cryofixation combined with FS has significantly enhanced our ability to visualize structural details in a state closer to their native state (119–121), including entirely preserved acidocalcisomes in *T. cruzi*, revealing both the highly dense core and the surrounding membrane with its phospholipid bilayer (72). Over the past 20 years, this method has been increasingly applied, particularly in conjunction with volume microscopy techniques in the field of protozoology (121–127). Unlike single ultrathin or cryoultrathin sections that capture only two-dimensional images, these techniques allow for the detailed visualization of complex cellular and subcellular structures within a given volume, offering a better comprehension of spatial relationships (128–130).

Electron tomography effectively overcomes the resolution limitations inherent in other techniques by using virtual sectioning in semi-ultrathin sections (~ 200 nm) during tomogram reconstruction. This process enables the automated acquisition of high-resolution images with excellent lateral and z-axis resolution (128, 131). The ability to perform high-resolution volumetric imaging and reconstruction has opened up new opportunities to observe rarely visualized dynamic cellular events, such as acidocalcisome interactions with the contractile vacuole complex via membrane fusion (124, 132). This observation supports the role of acidocalcisomes in the osmoregulatory mechanism of *T. cruzi*, facilitating the transfer of ions and polyphosphates to the vacuole lumen and thereby increasing osmotic pressure within this organelle (63, 64, 132).

Even in ET of FS cells, acidocalcisomes displayed an empty matrix, with residual electron-dense material localized at the inner membrane surface (124). This phenomenon may have resulted from contact of the sections with water during the ultramicrotomy step prior to tomogram acquisition. This issue particularly affects diffusible cellular components, such as the ion-rich core of acidocalcisomes, which can be extracted from the section in regions exposed to water (113).

Advances in the elemental detection methods

Determination of ion content, distribution, and concentration within cells is essential for understanding various cellular processes. Among the techniques used for this purpose, electron microscopy-based methods, particularly electron energy-loss spectroscopy (EELS) and related methods, and energy-dispersive X-ray spectroscopy (EDS), have been proven to be the most effective methods for high-resolution, subcellular *in situ* visualization of ion distribution within cells and organelles, such as acidocalcisomes.

Electron energy-loss spectroscopy (EELS) is carried out using a transmission electron microscope or a scanning transmission electron microscope (STEM) equipped with an energy filter (energy-filtering transmission electron microscope [EFTEM]). In both cases, the technique measures the electron energy loss after the interaction of the primary electron beam with the sample and can be applied on thin films of plunge-frozen samples using a cryoelectron microscope (133). EELS can provide information more than just elemental composition, such as thickness, quantitative information, bound elements, and oxidation states, and be combined with electron tomography to 3D elemental mapping of ions with high sensitivity at subnanometer resolution, which is particularly of great interest in the biological field (134, 135). Despite its superior sensitivity and spatial resolution for detecting elements at very low concentrations (90, 134, 136), its application to biological samples remains challenging due to their susceptibility to beam damage. Nevertheless, numerous studies have employed EELS methods to characterize acidocalcisomes in different protozoan parasites. Most of these studies have focused on elemental composition analysis to understand physiological aspects (137, 138) or ultrastructural analysis with contrast tuning (72, 74, 139–141).

Electron probe X-ray microanalysis (EPXMA), also known as energy-dispersive spectroscopy (EDS), has been used for decades as a powerful method to study the composition, distribution, and quantification of chemical elements in various materials and biological samples (142–146). This technique can detect simultaneously nearly all elements present in the sample with the advantage of correlating composition with ultrastructural details. The principle of X-ray microanalysis is based on the generation of X rays when the electron beam interacts with the atoms of the sample. X rays are collected by a detector positioned close to the sample, and a system classifies them by energy to produce a spectrum. The resulting histogram provides qualitative and quantitative information about the elemental composition of the sample (142). X-ray microanalysis can be performed using either scanning or transmission electron microscopy (S/TEM), enabling the analysis of samples ranging from thin sections to whole cells. Since diffusible elements are often lost during conventional preparation methods, the gold standard for X-ray microanalysis includes cryofixation techniques, such as plunge freezing, cryosectioning for thick samples, and freeze-drying as previously discussed (142, 147). These methodologies have been key tools for determining the chemical composition and, consequently, a better understanding about physiological processes that take place in acidocalcisomes of different organisms (43, 147, 148).

Advances in multi-detector systems, or array configurations, integrated with STEM have significantly enhanced detection sensitivity, enabling faster and more precise elemental mapping (149, 150). Recently, our group demonstrated the presence of ion nanodomains within acidocalcisomes of whole *T. cruzi* cells using a workflow that combined cryofixation with elemental mapping on a STEM microscope equipped with a system of four integrated EDS detectors and electron tomography for 3D elemental

mapping. This study revealed a self-excluding pattern of cationic elements, such as magnesium and calcium (Fig. 1E) (91). These findings highlighted distinct features of the acidocalcisome core, providing the first evidence for a mechanism of formation of biomolecular condensates within an organelle, thus contributing to our understanding of the physiology of this organelle that may expand to other cell types. Moreover, ongoing advancements in X-ray mapping techniques continue to improve resolution and sensitivity, enabling exploration of three-dimensional elemental distributions (151). When integrated with cryo-EM, these innovations may significantly expand the scope of analytical studies on soft materials, with potential impact in various biological samples, including molecules.

THE ACIDOCALCISOME IN THE AGE OF THE RESOLUTION REVOLUTION

The “resolution revolution” of biological sample imaging has been fueled by significant advancements in cryo-transmission electron microscopy (TEM), particularly through the development of microscopes operating at 300 kV and equipped with field emission guns (FEGs). These microscopes generate highly coherent electron beams with increased penetration power, enabling high-resolution imaging (152). Additionally, the introduction of direct electron detectors (DEDs) has transformed cryo-EM by enabling individual electron event detection and dose distribution across multiple frames. This technology allows motion correction, enhances imaging flexibility, and significantly improves image quality (153, 154).

To counteract the inherent low signal-to-noise ratio typically found when imaging biological samples—due to the use of low-dose imaging techniques—energy filters have been employed to remove electrons that have suffered energy loss and contribute to chromatic aberration. In this so-called zero-loss imaging, only unscattered and elastically scattered electrons that come through the objective aperture are retained, improving image contrast (155–157). Further contrast enhancement can be achieved by defocusing or with the use of phase plates (158, 159).

Advancements in cryo-focused ion beam scanning electron microscopy (cryo-FIB SEM) have significantly contributed to the improvement of resolution in biological cryo-EM. Cryo-lamellae preparation and lift-out approaches enable precise thinning and preparation of samples for high-resolution structural analysis, overcoming limitations of traditional methods like CEMOVIS (14, 31, 160, 161). By preserving structural integrity and minimizing artifacts, cryo-FIB SEM enhances sample quality and supports clearer imaging, making it an invaluable tool for cryo-ET (14, 160, 162). Additionally, combining cryo dual-beam microscopy with cryo-fluorescence microscopy allows precise localization of specific structures or molecules within complex samples. This integration is particularly useful for physiological studies, offering detailed contextual insights into biological systems (163–166).

Although there are no published cryo-EM studies fully dedicated to investigating the acidocalcisome yet, evidence suggests that these new technologies could be important tools to improve our understanding of this organelle and its physiological functions.

To investigate the impact of *T. brucei* flagellar movement on the parasite structure, Sun et al. (28) used cryo-ET to observe whole zoid cells (anucleate cells) displaying structural modifications in the flagellar attachment zone. Although not explicitly identified by the authors, numerous electron-dense granules were described, ranging from 100 to 350 nm in diameter, resembling the well-characterized acidocalcisome in trypanosomatids (28). Those electron-dense granules were observed in close contact with the mitochondria. Similarly, the interaction between mitochondria and acidocalcisomes has been suggested in *Chlamydomonas*, *T. brucei*, and *T. cruzi*. Indirect evidence, primarily based on the proximity of these organelles in ultrathin sections and super-resolution fluorescence microscopy images, has been documented (59, 72, 167, 168). In addition to identifying contact sites between these organelles, studies in *T. brucei* have implicated the IP3 receptor (located on acidocalcisome membrane), the voltage-dependent anion channel (VDAC; on the outer mitochondrial membrane), and the mitochondrial calcium

uniporter (MCU; on the inner mitochondrial membrane) as mediators of Ca^{2+} ion transfer from the acidocalcisome to the mitochondrion (168, 169). In *T. cruzi*, deletion of the receptor TcIP3R disrupted the parasite's metabolism by decreasing mitochondrial Ca^{2+} uptake, which inhibited O_2 consumption and oxidative phosphorylation (59).

Although calcium transfer to mitochondria in eukaryotes is well-established, research on the mechanism, quantity, and bioavailability of calcium within the mitochondria remains limited mainly due to the challenges in preserving ions for imaging and detection, as previously discussed. However, this scenario seems to be changing with the recent cryo-ET improvements. A study on osteoblasts subjected to high-pressure freezing and freeze substitution, followed by EDX, identified electron-dense granules in the mitochondrial matrix composed of calcium phosphate (170). Later, a similar result was observed in fibroblasts through cryo-ET in scanning transmission electron microscopy (STEM) combined with EDX, showing amorphous and dense granules dispersed in the mitochondrial matrix also composed of calcium phosphate (30). Given the widespread presence of acidocalcisomes and acidocalcisome-like structures across diverse biological groups, these findings further reinforce the role of this organelle not only in the storage of essential ions but also in its interactions with organelles, such as mitochondria and its involvement in various physiological processes, including bioenergetics.

Cryofixed whole cells of *T. cruzi* analyzed by single-image cryo-EM and cryo-ET revealed acidocalcisomes with varying electron-dense core patterns (91). Some displayed a fully filled electron-dense matrix, while others appeared only partially filled (Fig. 2A and B) (91). Similarly, partially filled acidocalcisomes were observed in *Chlamydomonas* using cryo-FIB-SEM lamella analyzed by cryo-ET (33). The use of cryo-FIB-SEM lamella on sample preparation minimizes the artifacts commonly associated with traditional sectioning techniques (Fig. 2C), allowing for high-resolution visualization of ion-rich subcellular compartments in their hydrated state (Fig. 2D). This approach opens new paths for studying the ultrastructure and function of acidocalcisomes under near-native conditions. Preliminary data from cryo-ET analysis of acidocalcisomes revealed a distinct texture in the matrix, characterized by “fiber-like” regions (Fig. 2E). When modeled, the fibers exhibit dimensions very similar to those expected for polyPs, likely corresponding to the visualization of aggregates of polyphosphate molecules (Fig. 2F). Molecular fitting analysis, considering polyphosphate dimensions and interactions with divalent ions (91), aligns well with these observations and the measurements obtained from cryo-ET models (Fig. 2G). All evidence points to the possibility that we are observing polyphosphate aggregates *in situ* (Movie S1).

The variability in acidocalcisome matrix patterns observed in hydrated cells at high resolution underscores the need to reconsider the prevalent assumption that acidocalcisomes, in their native state, consistently feature a fully electron-dense matrix, and that any deviation from this morphology is merely a technical artifact. Moving beyond this assumption opens the possibility that a partially filled matrix could represent a native physiological state, potentially indicative of ion mobilization for maintaining homeostasis or as a stress response. Previous studies have already indicated substantial ion mobilization and ultrastructural dynamics within this organelle. In *Leishmania amazonensis*, a polymorphic acidocalcisome core was documented, showing dynamic changes in elemental composition and concentration in response to varying extracellular nutritional conditions, suggesting a high degree of ion storage shifts and mobility that result in ultrastructural changes (74). Similar ultrastructural diversity in the acidocalcisome matrix has also been reported in *Phytomonas françai* (53).

Thus, if the observed matrix patterns in acidocalcisomes represent distinct physiological stages of this organelle, could intermediate stages of ion mobilization be captured using cryo-EM? Furthermore, is it possible to visualize the nanodomains described within the acidocalcisome core with the latest advancements in cryomicroscopy? Recent findings suggest a promising future in this direction (Fig. 2).

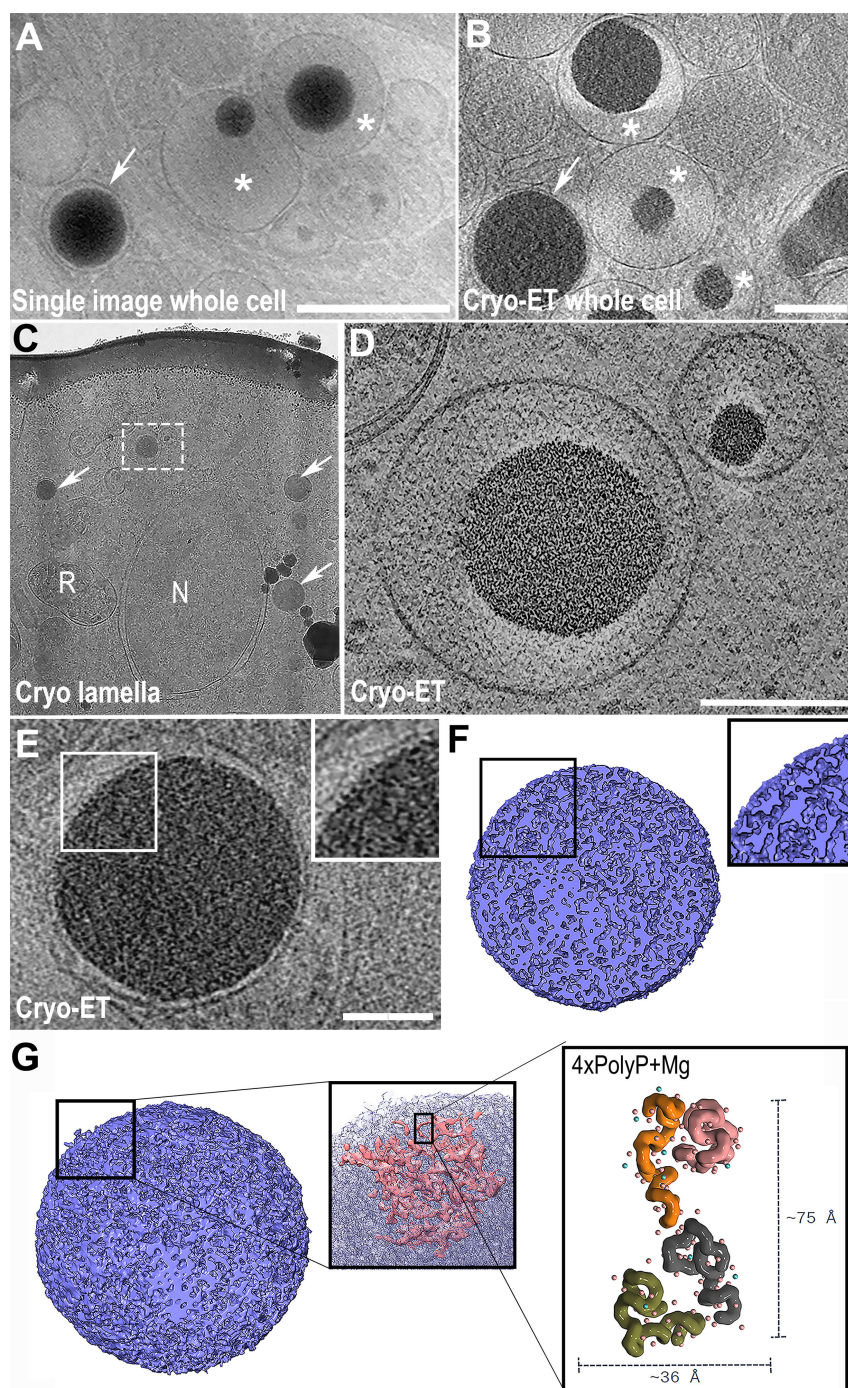


FIG 2 Visualization of acidocalcisomes in *T. cruzi* using cryo-EM and cryo-ET. (A and B) A single image and a virtual section from a whole cell tomogram, respectively. Both images show different patterns of acidocalcisome structure, the fully loaded matrix containing a well-preserved electrodense core (arrows) and the partially filled matrix with cores of different diameters (asterisks). In these images, the surrounding and intracellular interactions with the acidocalcisomes can be clearly observed. Scale bar = 500 and 200 nm, respectively. (C) TEM image of a ~200 nm lamella from an epimastigote form of *T. cruzi*. To minimize beam damage and acquire an overview for a search map, images of lamellae are initially acquired at low magnification, which reduces the signal-to-noise ratio (SNR). The nucleus (N), reservosomes (R), and acidocalcisomes are visible, with their matrix either fully (arrows) or partially filled (dotted square). (D) Cryo-ET virtual section of the acidocalcisomes from the dotted square region in panel (Continued on next page)

Fig 2 (Continued)

A, showing both the membranes and electrodense cores with high resolution. Scale bar = 200 nm. (E) Cryo-ET of whole cell virtual section, displaying fine details of the acidocalcisome matrix texture (inset), potentially representing the *in situ* observation of aggregates of polyphosphate molecules. Scale bar = 100 nm. (F) 3D model based on the threshold of the acidocalcisome matrix shown in panel E. (G) The final 3D model reveals highly interconnected structures, which, when closely observed, resemble the conformation and size of polyphosphate chains in the presence of ions such as Mg^{2+} . Conformation models obtained from molecular dynamics based on four polyphosphate chains with 50 phosphates and magnesium over a 100 ns simulation are shown. (Panel A was reproduced from reference 91 with permission.)

A final question arising from this discussion is whether the high-resolution capabilities of cryo-EM could be effectively combined with elemental detection methods. The potential of such a combination could offer detailed ultrastructural information on acidocalcisomes in hydrated conditions, along with a comprehensive ion profile and mobilization—not only within the acidocalcisome matrix but also in interacting organelles, such as mitochondria and contractile vacuole. Capturing these dynamic processes in a near-native state could be instrumental in understanding the role of acidocalcisomes in parasite physiology

CONCLUSION AND FUTURE PERSPECTIVES

The use of cryo-EM to reveal new structural aspects of pathogens at the molecular level is expected to continue expanding in the coming years, provided that technological development investments remain strong. Just as correlative light electron microscopy (CLEM) has evolved to extend cryo-EM beyond mere morphological characterization, the integration of cryoelectron microscopy with elemental ion detection technologies holds significant potential to push existing boundaries. Many of the tools required to make this combination a reality are already available. On one hand, transmission electron microscopes equipped with sensitive multi-detector systems and capable of running electron tomograms, including cryo-ET, are accessible, though improvements in the column design could help address current limitations in angular range and the use of cryo-holders. On the other hand, to enhance contrast, most 300 kV TEMs are now equipped with energy filters. Despite being the most widely used instrument for high-end cryo-EM, the current generation equipment has significant limitations in fully leveraging the electron energy loss spectrum, featuring slit aperture controls ranging from 1 to 500 eV, limiting its functionality primarily to zero-loss imaging. Expanding support for elemental detection through EELS and optimized contrast (tuning) for whole-cell analyses, particularly integrating the latest laser phase plate technologies, holds tremendous potential for advancing the field.

In addition to their role in cell physiology, the understanding of Ca^{2+} storage nanostructures and the modulation of their binding to the support matrix, such as polyphosphate in acidocalcisomes, modulated by pH variation, is also in line with technological research on calcium-based batteries (171). The structural investigation of acidocalcisomes, in this sense, may also suggest polymers similar to polyphosphates as efficient matrices for the storage and release of divalent ions for these batteries, such as Ca^{2+} and Mg^{2+} , which are much more abundant than the monovalent lithium.

Regardless of the specific advancements in cryo-EM future, its contribution to biological sciences and the study of infectious diseases remains undeniable. Expanding the application of cryo-EM has the potential to deepen our understanding of protozoan parasite ultrastructure and physiology, offering new perspectives for therapeutic development.

ACKNOWLEDGMENTS

The authors thank Msc Adélia Belém and Vania Vieira for their invaluable work on sample preparation and cryoEM imaging and data acquisition.

This work was supported by funds from Fundação Carlos Chagas Filho de Amparo à Pesquisa do Estado do Rio de Janeiro (FAPERJ) Grant Numbers E-26/200.008/2020, E-26/210.285/2023, E-26/201.099/2021, and E-26/210.739/2021; Conselho Nacional de Desenvolvimento Científico e Tecnológico, CNPq-Brazil, Grant numbers 314388/2021-4 and 315574/2021-6; Coordenação de Aperfeiçoamento de Profissionais de Nível Superior, CAPES-Brazil; and Financiadora de Estudos e Projetos, FINEP-Brazil. This project is part of the National Institute of Science and Technology in Structural Biology and Bioimaging-INBEB, funded by the Brazilian government.

AUTHOR AFFILIATIONS

¹Laboratório de Ultraestrutura Celular Hertha Meyer, Centro de Pesquisa em Medicina de Precisão, Instituto de Biofísica Carlos Chagas Filho and Centro Nacional de Biologia Estrutural e Bioimagem, Universidade Federal do Rio de Janeiro, Rio de Janeiro, Brazil

²Instituto Nacional de Ciência e Tecnologia em Biologia Estrutural e Bioimagem—Universidade Federal do Rio de Janeiro, Rio de Janeiro, Brazil

³Institut Pasteur, Paris, France

⁴Plataforma de Microscopia Eletrônica Rudolf Barth, Instituto Oswaldo Cruz–Fiocruz, Rio de Janeiro, Brazil

⁵Laboratório de Modelagem e Dinâmica Molecular, Instituto de Biofísica Carlos Chagas Filho, Universidade Federal do Rio de Janeiro, Rio de Janeiro, Brazil

⁶Centro Multiusuário para Análise de Fenômenos Biomédicos, Universidade do Estado do Amazonas, Amazonas, Brazil

AUTHOR ORCIDs

Ingrid Augusto  <http://orcid.org/0000-0003-0651-0899>

Kildare Miranda  <http://orcid.org/0000-0001-9799-773X>

AUTHOR CONTRIBUTIONS

Ingrid Augusto, Conceptualization, Data curation, Formal analysis, Investigation, Methodology, Validation, Visualization, Writing – original draft, Writing – review and editing | Moara Lemos, Formal analysis, Investigation, Methodology, Writing – original draft, Writing – review and editing | Wendell Girard-Dias, Data curation, Investigation, Writing – original draft | José de Anchieta Oliveira Filho, Data curation, Formal analysis, Investigation, Methodology, Visualization, Writing – original draft | Pedro G. Pascutti, Conceptualization, Data curation, Investigation, Supervision, Writing – review and editing | Wanderley de Souza, Formal analysis, Funding acquisition, Investigation, Writing – review and editing | Kildare Miranda, Conceptualization, Data curation, Formal analysis, Funding acquisition, Investigation, Methodology, Project administration, Resources, Supervision, Visualization, Writing – original draft, Writing – review and editing

ADDITIONAL FILES

The following material is available [online](#).

Supplemental Material

Legend (mBio01662-24-S0001.docx). Supplemental movie legend.

Movie S1 (mBio01662-24-S0002.mp4). *In situ* visualization of an acidocalcisome by cryo-ET.

REFERENCES

- Weissenberger G, Henderikx RJM, Peters PJ. 2021. Understanding the invisible hands of sample preparation for cryo-EM. *Nat Methods* 18:463–471. <https://doi.org/10.1038/s41592-021-01130-6>
- Turk M, Baumeister W. 2020. The promise and the challenges of cryo-electron tomography. *FEBS Lett* 594:3243–3261. <https://doi.org/10.1002/1873-3468.13948>
- Bäuerlein FJB, Fernández-Busnadiego R, Baumeister W. 2020. Investigating the structure of neurotoxic protein aggregates inside cells. *Trends Cell Biol* 30:951–966. <https://doi.org/10.1016/j.tcb.2020.08.007>
- Erdmann PS, Plitzko JM, Baumeister W. 2018. Addressing cellular compartmentalization by *in situ* cryo-electron tomography. *Curr Opin Colloid & Interface Sci* 34:89–99. <https://doi.org/10.1016/j.cocis.2018.05.003>
- Chakraborty S, Jasmin M, Baumeister W. 2020. Three-dimensional organization of the cytoskeleton: a cryo-electron tomography perspective. *Protein Sci* 29:1302–1320. <https://doi.org/10.1002/pro.3858>
- Bodakuntla S, Kuhn CC, Biertümpfel C, Mizuno N. 2023. Cryo-electron microscopy in the fight against COVID-19-mechanism of virus entry. *Front Mol Biosci* 10:1252529. <https://doi.org/10.3389/fmolb.2023.1252529>
- Xu C, Han W, Cong Y. 2023. Cryo-EM and cryo-ET of the spike, virion, and antibody neutralization of SARS-CoV-2 and VOCs. *Curr Opin Struct Biol* 82:102664. <https://doi.org/10.1016/j.sbi.2023.102664>
- Liu C, Mendonça L, Yang Y, Gao Y, Shen C, Liu J, Ni T, Ju B, Liu C, Tang X, Wei J, Ma X, Zhu Y, Liu W, Xu S, Liu Y, Yuan J, Wu J, Liu Z, Zhang Z, Liu L, Wang P, Zhang P. 2020. The architecture of inactivated SARS-CoV-2 with postfusion spikes revealed by Cryo-EM and Cryo-ET. *Structure* 28:1218–1224. <https://doi.org/10.1016/j.str.2020.10.001>
- Klein S, Cortese M, Winter SL, Wachsmuth-Melm M, Neufeldt CJ, Cerikan B, Stanifer ML, Boulant S, Bartenschlager R, Chlanda P. 2020. SARS-CoV-2 structure and replication characterized by *in situ* cryo-electron tomography. *Nat Commun* 11:5885. <https://doi.org/10.1038/s41467-020-19619-7>
- Shepherd DC, Dalvi S, Ghosal D. 2022. From cells to atoms: Cryo-EM as an essential tool to investigate pathogen biology, host-pathogen interaction, and drug discovery. *Mol Microbiol* 117:610–617. <https://doi.org/10.1111/mmi.14820>
- Asarnow D, Becker VA, Bobe D, Dubbledam C, Johnston JD, Kopylov M, Lavoie NR, Li Q, Mattingly JM, Mendez JH, Paraaan M, Turner J, Upadhye V, Walsh RM, Gupta M, Eng ET. 2023. Recent advances in infectious disease research using cryo-electron tomography. *Front Mol Biosci* 10:1296941. <https://doi.org/10.3389/fmolb.2023.1296941>
- Theveny LM, Mageswaran SK, Chen WD, Martinez M, Guérin A, Chang YW. 2022. Parasitology meets cryo-electron tomography - exciting prospects await. *Trends Parasitol* 38:365–378. <https://doi.org/10.1016/j.pt.2022.01.006>
- Gui L, O'Shaughnessy WJ, Cai K, Reetz E, Reese ML, Nicastro D. 2023. Cryo-tomography reveals rigid-body motion and organization of apicomplexan invasion machinery. *Nat Commun* 14:1–14. <https://doi.org/10.1038/s41467-023-37327-w>
- Bisson C, Hecksel CW, Gilchrist JB, Carbajal MA, Fleck RA. 2021. Preparing lamellae from vitreous biological samples using a dual-beam scanning electron microscope for cryo-electron tomography. *J Vis Exp* 174. <https://doi.org/10.3791/62350>
- Mageswaran SK, Guérin A, Theveny LM, Chen WD, Martinez M, Lebrun M, Striepen B, Chang YW. 2021. *In situ* ultrastructures of two evolutionarily distant apicomplexan rhoptry secretion systems. *Nat Commun* 12:4983. <https://doi.org/10.1038/s41467-021-25309-9>
- Martinez M, Mageswaran SK, Guérin A, Chen WD, Thompson CP, Chavin S, Soldati-Favre D, Striepen B, Chang YW. 2023. Origin and arrangement of actin filaments for gliding motility in apicomplexan parasites revealed by cryo-electron tomography. *Nat Commun* 14:1–16. <https://doi.org/10.1038/s41467-023-40520-6>
- Sun SY, Segev-Zarko L-A, Pintilie GD, Kim CY, Staggers SR, Schmid MF, Egan ES, Chiu W, Boothroyd JC. 2024. Cryogenic electron tomography reveals novel structures in the apical complex of *Plasmodium falciparum*. *MBio* 15:e0286423. <https://doi.org/10.1128/mbio.02864-23>
- Sun S-Y, Segev-Zarko LA, Chen M, Pintilie GD, Schmid MF, Ludtke SJ, Boothroyd JC, Chiu W. 2022. Cryo-ET of *Toxoplasma* parasites gives subnanometer insight into tubulin-based structures. *Proc Natl Acad Sci USA* 119:e2111661119. <https://doi.org/10.1073/pnas.2111661119>
- Li Z, Du W, Yang J, Lai DH, Lun ZR, Guo Q. 2023. Cryo-electron tomography of *Toxoplasma gondii* indicates that the conoid fiber may be derived from microtubules. *Adv Sci (Weinh)* 10:e2206595. <https://doi.org/10.1002/adv.202206595>
- Dos Santos Pacheco N, Tell I Puig A, Guérin A, Martinez M, Maco B, Tosetti N, Delgado-Betancourt E, Lunghi M, Striepen B, Chang Y-W, Soldati-Favre D. 2024. Sustained rhoptry docking and discharge requires *Toxoplasma gondii* intraconoidal microtubule-associated proteins. *Nat Commun* 15:379. <https://doi.org/10.1038/s41467-023-44631-y>
- Segev-Zarko LA, Dahlberg PD, Sun SY, Pelt DM, Kim CY, Egan ES, Sethian JA, Chiu W, Boothroyd JC. 2022. Cryo-electron tomography with mixed-scale dense neural networks reveals key steps in deployment of *Toxoplasma* invasion machinery. *PNAS Nexus* 1:pgac183. <https://doi.org/10.1093/pnasnexus/pgac183>
- Li Z, Guo Q, Zheng L, Ji Y, Xie YT, Lai DH, Lun ZR, Suo X, Gao N. 2017. Cryo-EM structures of the 80S ribosomes from human parasites *Trichomonas vaginalis* and *Toxoplasma gondii*. *Cell Res* 27:1275–1288. <https://doi.org/10.1038/cr.2017.104>
- Majumdar S, Emmerich A, Krakovska S, Mandava CS, Svärd SG, Sanyal S. 2023. Insights into translocation mechanism and ribosome evolution from cryo-EM structures of translocation intermediates of *Giardia intestinalis*. *Nucleic Acids Res* 51:3436–3451. <https://doi.org/10.1093/nar/gkad176>
- Schwartz CL, Dawson SC, Hoenger A. 2008. Cryo-electron tomography of isolated cytoskeletons of *Giardia intestinalis*. *Microsc Microanal* 14:1304–1305. <https://doi.org/10.1017/S1543192708085462>
- Sato S, Takizawa Y, Hoshikawa F, Dacher M, Tanaka H, Tachiwana H, Kujirai T, Ikura Y, Ho CH, Adachi N, Patwal I, Flaus A, Kurumizaka H. 2021. Cryo-EM structure of the nucleosome core particle containing *Giardia lamblia* histones. *Nucleic Acids Res* 49:8934–8946. <https://doi.org/10.1093/nar/gkab644>
- Brown JR, Schwartz CL, Heumann JM, Dawson SC, Hoenger A. 2016. A detailed look at the cytoskeletal architecture of the *Giardia lamblia* ventral disc. *J Struct Biol* 194:38–48. <https://doi.org/10.1016/j.jsb.2016.01.011>
- Cook AD, Roberts AJ, Atherton J, Tewari R, Topf M, Moores CA. 2021. Cryo-EM structure of a microtubule-bound parasite kinesin motor and implications for its mechanism and inhibition. *J Biol Chem* 297:101063. <https://doi.org/10.1016/j.jbc.2021.101063>
- Sun SY, Kaelber JT, Chen M, Dong X, Nematbakhsh Y, Shi J, Dougherty M, Lim CT, Schmid MF, Chiu W, He CY. 2018. Flagellum couples cell shape to motility in *Trypanosoma brucei*. *Proc Natl Acad Sci USA* 115:E5916–E5925. <https://doi.org/10.1073/pnas.1722618115>
- Trépot S. 2020. *In situ* structural analysis of the flagellum attachment zone in *Trypanosoma brucei* using cryo-scanning transmission electron tomography. *J Struct Biol* 4:100033. <https://doi.org/10.1016/j.jsbx.2020.100033>
- Wolf SG, Mutsaers Y, Dadosh T, Ilani T, Lansky Z, Horowitz B, Rubin S, Elbaum M, Fass D. 2017. 3D visualization of mitochondrial solid-phase calcium stores in whole cells. *Elife* 6:e29929. <https://doi.org/10.7554/eLife.29929>
- Buckley G, Gervinskis G, Taveneau C, Venugopal H, Whisstock JC, de Marco A. 2020. Automated cryo-lamella preparation for high-throughput *in-situ* structural biology. *J Struct Biol* 210:107488. <https://doi.org/10.1016/j.jsb.2020.107488>
- Höög JL, Bouchet-Marquis C, McIntosh JR, Hoenger A, Gull K. 2012. Cryo-electron tomography and 3-D analysis of the intact flagellum in *Trypanosoma brucei*. *J Struct Biol* 178:189–198. <https://doi.org/10.1016/j.jsb.2012.01.009>
- Schaffer M, Mahamid J, Engel BD, Laugks T, Baumeister W, Plitzko JM. 2017. Optimized cryo-focused ion beam sample preparation aimed at *in situ* structural studies of membrane proteins. *J Struct Biol* 197:73–82. <https://doi.org/10.1016/j.jsb.2016.07.010>
- Zhang J, Wang H, Imhof S, Zhou X, Liao S, Atanasov I, Hui WH, Hill KL, Zhou ZH. 2021. Structure of the trypanosome paraflagellar rod and insights into non-planar motility of eukaryotic cells. *Cell Discov* 7. <https://doi.org/10.1038/s41421-021-00281-2>
- Liu Z, Gutierrez-Vargas C, Wei J, Grassucci RA, Ramesh M, Espina N, Sun M, Tutuncuoglu B, Madison-Antenucci S, Woolford JL, Tong L, Frank J.

2016. Structure and assembly model for the *Trypanosoma cruzi* 60S ribosomal subunit. *Proc Natl Acad Sci USA* 113:12174–12179. <https://doi.org/10.1073/pnas.1614594113>
36. Imhof S, Zhang J, Wang H, Bui KH, Nguyen H, Atanasov I, Hui WH, Yang SK, Zhou ZH, Hill KL. 2019. Cryo electron tomography with volta phase plate reveals novel structural foundations of the 96-nm axonemal repeat in the pathogen *Trypanosoma brucei* Elife 8:e52058. <https://doi.org/10.7554/eLife.52058>
 37. Docampo R. 2016. The origin and evolution of the acidocalcisome and its interactions with other organelles. *Mol Biochem Parasitol* 209:3–9. <https://doi.org/10.1016/j.molbiopara.2015.10.003>
 38. Meyer A. 1904. Orientierende untersuchung über die verbreitung, morphologie und chemie des volutins. *Bot Zeit* 62:113–153.
 39. Rosenberg H. 1966. The isolation and identification of “volutin” granules from Tetrahymena. *Exp Cell Res* 41:397–410. [https://doi.org/10.1016/S0014-4827\(66\)80147-7](https://doi.org/10.1016/S0014-4827(66)80147-7)
 40. Erdmann R. 1910. Kern und metachromatische körner bei sarkosporiden. *Arch Protistenkd* 20:239–243.
 41. Swellengrebel N. 1908. La volutine chez les Trypanosomes. *CR Soc Biol* 64:38–43.
 42. Wiame JM. 1947. Étude d'une substance polyphosphorée, basophile et métachromatique chez les levures. *Biochim Biophys Acta* 1:234–255. [https://doi.org/10.1016/0006-3002\(47\)90137-6](https://doi.org/10.1016/0006-3002(47)90137-6)
 43. Docampo R, de Souza W, Miranda K, Rohloff P, Moreno SNJ. 2005. Acidocalcisomes - conserved from bacteria to man. *Nat Rev Microbiol* 3:251–261. <https://doi.org/10.1038/nrmicro1097>
 44. Docampo R, Scott DA, Vercesi AE, Moreno SNJ. 1995. Intracellular Ca²⁺ storage in acidocalcisomes of *Trypanosoma cruzi*. *Biochem J* 310:1005–1012. <https://doi.org/10.1042/bj3101005>
 45. Vercesi AE, Moreno SNJ, Docampo R. 1994. Ca²⁺/H⁺ exchange in acidic vacuoles of *Trypanosoma brucei*. *Biochem J* 304 (Pt 1):227–233. <https://doi.org/10.1042/bj3040227>
 46. Ruiz FA, Lea CR, Oldfield E, Docampo R. 2004. Human platelet dense granules contain polyphosphate and are similar to acidocalcisomes of bacteria and unicellular eukaryotes. *J Biol Chem* 279:44250–44257. <https://doi.org/10.1074/jbc.M406261200>
 47. Ruiz FA, Marchesini N, Seufferheld M, Docampo R. 2001. The polyphosphate bodies of *Chlamydomonas reinhardtii* possess a proton-pumping pyrophosphatase and are similar to acidocalcisomes. *J Biol Chem* 276:46196–46203. <https://doi.org/10.1074/jbc.M105268200>
 48. Marchesini N, Luo S, Rodrigues CO, Moreno SNJ, Docampo R. 2000. Acidocalcisomes and a vacuolar H⁺-pyrophosphatase in malaria parasites. *Biochem J* 347 Pt 1:243–253.
 49. Miranda K, de Souza W, Plattner H, Hentschel J, Kawazoe U, Fang J, Moreno SNJ. 2008. Acidocalcisomes in Apicomplexan parasites. *Exp Parasitol* 118:2–9. <https://doi.org/10.1016/j.exppara.2007.07.009>
 50. Moreno SNJ, Zhong L. 1996. Acidocalcisomes in *Toxoplasma gondii* tachyzoites. *Biochem J* 313 (Pt 2):655–659. <https://doi.org/10.1042/bj3130655>
 51. Lemos M, Fermino BR, Simas-Rodrigues C, Hoffmann L, Silva R, Camargo EP, Teixeira MMG, Souto-Padrón T. 2015. Phylogenetic and morphological characterization of trypanosomes from Brazilian armoured catfishes and leeches reveal high species diversity, mixed infections and a new fish trypanosome species. *Parasites Vectors* 8:573. <https://doi.org/10.1186/s13071-015-1193-7>
 52. Yurchenko VY, Lukes J, Jirku M, Zeledón R, Maslov DA. 2006. *Leptomonas costaricensis* sp. n. (Kinetoplastea: Trypanosomatidae), a member of the novel phylogenetic group of insect trypanosomatids closely related to the genus *Leishmania*. *Parasitology* 133:537–546. <https://doi.org/10.1017/S0031182006000746>
 53. Miranda K, Rodrigues CO, Hentschel J, Vercesi A, Plattner H, De SW, Docampo R. 2004. Acidocalcisomes of phytomonas françai possess distinct morphological characteristics and contain iron:647–655. <https://doi.org/10.1017/S1431927604040887>
 54. Hill JE, Scott DA, Luo S, Docampo R. 2000. Cloning and functional expression of a gene encoding a vacuolar-type proton-translocating pyrophosphatase from *Trypanosoma cruzi*. *Biochem J* 351:281–288. <https://doi.org/10.1042/0264-6021:3510281>
 55. Lu HG, Zhong L, de Souza W, Benchimol M, Moreno S, Docampo R. 1998. Ca²⁺ content and expression of an acidocalcisomal calcium pump are elevated in intracellular forms of *Trypanosoma cruzi*. *Mol Cell Biol* 18:2309–2323. <https://doi.org/10.1128/MCB.18.4.2309>
 56. Huang G, Ulrich PN, Storey M, Johnson D, Tischer J, Tovar JA, Moreno SNJ, Orlando R, Docampo R. 2014. Proteomic analysis of the acidocalcisome, an organelle conserved from bacteria to human cells. *PLoS Pathog* 10:e1004555. <https://doi.org/10.1371/journal.ppat.1004555>
 57. Huang G, Bartlett PJ, Thomas AP, Moreno SNJ, Docampo R. 2013. Acidocalcisomes of *Trypanosoma brucei* have an inositol 1,4,5-trisphosphate receptor that is required for growth and infectivity. *Proc Natl Acad Sci USA* 110:1887–1892. <https://doi.org/10.1073/pnas.1216955110>
 58. Potapenko E, Negrão NW, Huang G, Docampo R. 2019. The acidocalcisome inositol-1,4,5-trisphosphate receptor of *Trypanosoma brucei* is stimulated by luminal polyphosphate hydrolysis products. *J Biol Chem* 294:10628–10637. <https://doi.org/10.1074/jbc.RA119.007906>
 59. Chiurillo MA, Lander N, Vercesi AE, Docampo R. 2020. IP₃ receptor-mediated Ca²⁺ release from acidocalcisomes regulates mitochondrial bioenergetics and prevents autophagy in *Trypanosoma cruzi*. *Cell Calcium* 92:102284. <https://doi.org/10.1016/j.ceca.2020.102284>
 60. Lander N, Chiurillo MA, Storey M, Vercesi AE, Docampo R. 2016. CRISPR/Cas9-mediated endogenous C-terminal tagging of *Trypanosoma cruzi* genes reveals the acidocalcisome localization of the inositol 1,4,5-trisphosphate receptor. *J Biol Chem* 291:25505–25515. <https://doi.org/10.1074/jbc.M116.749655>
 61. Lander N, Ulrich PN, Docampo R. 2013. *Trypanosoma brucei* vacuolar transporter chaperone 4 (TbVtc4) is an acidocalcisome polyphosphate kinase required for *in vivo* infection. *J Biol Chem* 288:34205–34216. <https://doi.org/10.1074/jbc.M113.518993>
 62. Ulrich PN, Lander N, Kurup SP, Reiss L, Brewer J, Soares Medeiros LC, Miranda K, Docampo R. 2014. The acidocalcisome vacuolar transporter chaperone 4 catalyzes the synthesis of polyphosphate in insect-stages of *Trypanosoma brucei* and *T. cruzi*. *J Eukaryot Microbiol* 61:155–165. <https://doi.org/10.1111/jeu.12093>
 63. Montalvetti A, Rohloff P, Docampo R. 2004. A functional aquaporin co-localizes with the vacuolar proton pyrophosphatase to acidocalcisomes and the contractile vacuole complex of *Trypanosoma cruzi*. *J Biol Chem* 279:38673–38682. <https://doi.org/10.1074/jbc.M406304200>
 64. Docampo R. 2024. Advances in the cellular biology, biochemistry, and molecular biology of acidocalcisomes. *Microbiol Mol Biol Rev* 88:e0004223. <https://doi.org/10.1128/mmb.00042-23>
 65. Nolan DP, Voorheis HP. 2000. Hydrogen ion gradients across the mitochondrial, endosomal and plasma membranes in bloodstream forms of *Trypanosoma brucei* solving the three-compartment problem. *Eur J Biochem* 267:4601–4614. <https://doi.org/10.1046/j.1432-1327.2000.01476.x>
 66. Lemerrier G, Dutoya S, Luo S, Ruiz FA, Rodrigues CO, Baltz T, Docampo R, Bakalara N. 2002. A vacuolar-type H⁺-pyrophosphatase governs maintenance of functional acidocalcisomes and growth of the insect and mammalian forms of *Trypanosoma brucei*. *J Biol Chem* 277:37369–37376. <https://doi.org/10.1074/jbc.M204744200>
 67. Huang G, Vercesi AE, Docampo R. 2013. Essential regulation of cell bioenergetics in *Trypanosoma brucei* by the mitochondrial calcium uniporter. *Nat Commun* 4:2865. <https://doi.org/10.1038/ncomms3865>
 68. Docampo R, Vercesi AE. 1989. Characteristics of Ca²⁺ transport by *Trypanosoma cruzi* mitochondria *in situ*. *Arch Biochem Biophys* 272:122–129. [https://doi.org/10.1016/0003-9861\(89\)90202-6](https://doi.org/10.1016/0003-9861(89)90202-6)
 69. Lu HG, Zhong L, Chang KP, Docampo R. 1997. Intracellular Ca²⁺ pool content and signaling and expression of a calcium pump are linked to virulence in *Leishmania mexicana* amazonensis amastigotes. *J Biol Chem* 272:9464–9473. <https://doi.org/10.1074/jbc.272.14.9464>
 70. Hong-hermesdorf A, Miethke M, Gallaher SD, Kropat J, Dodani SC, Chan J, Barupala D, Domaille DW, Shirasaki DI, Loo JA, Weber PK, Pett-Ridge J, Stemmler TL, Chang CJ, Merchant SS. 2014. Subcellular metal imaging identifies dynamic sites of Cu accumulation in *Chlamydomonas*. *Nat Chem Biol* 10:1034–1042. <https://doi.org/10.1038/nchembio.1662>
 71. Corrêa A, Andrade L, Soares M. 2002. Elemental composition of acidocalcisomes of *Trypanosoma cruzi* bloodstream trypomastigote forms. *Parasitol Res* 88:875–880. <https://doi.org/10.1007/s00436-002-0670-z>
 72. Miranda K, Benchimol M, Docampo R, de Souza W. 2000. The fine structure of acidocalcisomes in *Trypanosoma cruzi*. *Parasitol Res* 86:373–384. <https://doi.org/10.1007/s004360050682>
 73. Miranda K, Docampo R, Grillo O, de Souza W. 2004. Acidocalcisomes of trypanosomatids have species-specific elemental composition. *Protist* 155:395–405. <https://doi.org/10.1078/1434461042650361>
 74. Miranda K, Docampo R, Grillo O, Franzen A, Attias M, Vercesi A, Plattner H, Hentschel J, de Souza W. 2004. Dynamics of polymorphism of

- acidocalcisomes in *Leishmania* parasites. *Histochem Cell Biol* 121:407–418. <https://doi.org/10.1007/s00418-004-0646-4>
75. Hayat MA. 1970. Principles and techniques of electron microscopy: biological applications. 1st ed
 76. Fraenkel-conrat H, Olcott HS. 1948. The reaction of formaldehyde with proteins; cross-linking between amino and primary amide or guanidyl groups. *J Am Chem Soc* 70:2673–2684. <https://doi.org/10.1021/ja01188a018>
 77. Tayri-Wilk T, Slavin M, Zamel J, Blass A, Cohen S, Motzik A, Sun X, Shalev DE, Ram O, Kalisman N. 2020. Mass spectrometry reveals the chemistry of formaldehyde cross-linking in structured proteins. *Nat Commun* 11:3128. <https://doi.org/10.1038/s41467-020-16935-w>
 78. Karnovsky MJ. 1965. A formaldehyde-glutaraldehyde fixative of high osmolality for use in electron-microscopy. *J Cell Biol* 27
 79. Zingsheim HP, Plattner H. 1976. Electron microscopic methods in membrane biology. *Methods Membrane Biol*:1–146. https://doi.org/10.1007/978-1-4757-5820-7_1
 80. Fox CH, Johnson FB, Whiting J, Roller PP. 1985. Formaldehyde fixation. *J Histochem Cytochem* 33:845–853. <https://doi.org/10.1177/33.8.3894502>
 81. Hayat MA. 1981. Fixation for electron microscopy. Academic Press.
 82. Penttilä A, Kalimo H, Trump BF. 1974. Influence of glutaraldehyde and/or osmium tetroxide on cell volume, ion content, mechanical stability, and membrane permeability of Ehrlich ascites tumor cells. *J Cell Biol* 63:197–214. <https://doi.org/10.1083/jcb.63.1.197>
 83. Rautiainen M, Collan Y, Kärjä J, Nuutinen J. 1987. Artifacts in ultrastructure of respiratory cilia caused by various fixation procedures and different types of handling. *ORL J Otorhinolaryngol Relat Spec* 49:193–198. <https://doi.org/10.1159/000275935>
 84. Olins DE, Wright EB. 1973. Glutaraldehyde fixation of isolated eucaryotic nuclei. evidence for histone-histone proximity. *J Cell Biol* 59:304–317. <https://doi.org/10.1083/jcb.59.2.304>
 85. Hopwood D. 1967. The behaviour of various glutaraldehydes on Sephadex G-10 and some implications for fixation. *Histochemie* 11:289–295. <https://doi.org/10.1007/BF00305805>
 86. Scott DA, Docampo R, Dvorak JA, Shi S, Leapman RD. 2000. Characterization of isolated acidocalcisomes of *Trypanosoma cruzi*. *J Biol Chem* 275:24215–24221. <https://doi.org/10.1074/jbc.M002454200>
 87. Mollenhauer HH. 1993. Artifacts caused by dehydration and epoxy embedding in transmission electron microscopy. *Microsc Res Tech* 26:496–512. <https://doi.org/10.1002/jemt.1070260604>
 88. Bozzola J, Russell L. 1992. Electron microscopy: principles and techniques for biologists Second. Jones and Bartlett Publishers.
 89. Hayat M. 1981. Principles and techniques of electron microscopy. In *Biological applications*
 90. Scott DA, Docampo R, Dvorak JA, Shi S, Leapman RD. 1997. *In situ* compositional analysis of acidocalcisomes in *Trypanosoma cruzi* 272:28020–28029. <https://doi.org/10.1074/jbc.272.44.28020>
 91. Girard-Dias W, Augusto I, Fernandes TVA, Pascutti PG, de Souza W, Miranda K. 2023. A spatially resolved elemental nanodomain organization within acidocalcisomes in *Trypanosoma cruzi* *Proc Natl Acad Sci USA* 120:e2300942120. <https://doi.org/10.1073/pnas.2300942120>
 92. Dubochet J, McDowell AW. 1981. Vitricification of pure water for electron microscopy. *J Microsc* 124:3–4. <https://doi.org/10.1111/j.1365-2818.1981.tb02483.x>
 93. Dubochet J, Lepault J, Freeman R, Berriman JA, Homo J - C. 1982. Electron microscopy of frozen water and aqueous solutions. *J Microsc* 128:219–237. <https://doi.org/10.1111/j.1365-2818.1982.tb04625.x>
 94. Passmore LA, Russo CJ. 2016. Specimen preparation for high-resolution Cryo-EM. *Methods Enzymol* 579:51–86. <https://doi.org/10.1016/bs.mie.2016.04.011>
 95. Luyet B, Gehenio P. 1940. The mechanism of injury and death by low temperature. *Biodynamica* 3:33–60.
 96. Sanchez RM, Zhang Y, Chen W, Dietrich L, Kudryashev M. 2020. Subnanometer-resolution structure determination *in situ* by hybrid subtomogram averaging - single particle cryo-EM. *Nat Commun* 11:3709. <https://doi.org/10.1038/s41467-020-17466-0>
 97. Lazić I, Wirix M, Leidl ML, de Haas F, Mann D, Beckers M, Pechnikova EV, Müller-Caspar K, Egoavil R, Bosch EGT, Sachse C. 2022. Single-particle cryo-EM structures from iDPC-STEM at near-atomic resolution. *Nat Methods* 19:1126–1136. <https://doi.org/10.1038/s41592-022-01586-0>
 98. Cheng J, Liu T, You X, Zhang F, Sui SF, Wan X, Zhang X. 2023. Determining protein structures in cellular lamella at pseudo-atomic resolution by GiSPA. *Nat Commun* 14. <https://doi.org/10.1038/s41467-023-36175-y>
 99. Moor H. 1987. Theory and practice of high pressure freezing, p 175–191. In *Cryotechniques in biological electron microscopy*. Springer, Berlin, Heidelberg.
 100. Dahl R, Staehelin LA. 1989. High - pressure freezing for the preservation of biological structure: theory and practice. *J Elec Microsc Tech* 13:165–174. <https://doi.org/10.1002/jemt.1060130305>
 101. Adrian M, Dubochet J, Lepault J, McDowell AW. 1984. Cryo-electron microscopy of viruses. *Nature* 308:32–36. <https://doi.org/10.1038/308032a0>
 102. Tivol WF, Briegel A, Jensen GJ. 2008. An improved cryogen for plunge freezing. *Microsc Microanal* 14:375–379. <https://doi.org/10.1017/S1431927608080781>
 103. Dobro MJ, Melanson LA, Jensen GJ, McDowell AW. 2010. Plunge freezing for electron cryomicroscopy. *Methods Enzymol* 481:63–82. [https://doi.org/10.1016/S0076-6879\(10\)81003-1](https://doi.org/10.1016/S0076-6879(10)81003-1)
 104. D'Imprima E, Fung HKH, Zagorij I, Mahamid J. 2024. Cryogenic preparations of biological specimens for cryo-electron tomography. https://doi.org/10.1007/978-3-031-51171-4_3
 105. Vanhecke D, Graber W, Studer D. 2008. Close-to-native ultrastructural preservation by high pressure freezing. *Methods Cell Biol* 88:151–164. [https://doi.org/10.1016/S0091-679X\(08\)00409-3](https://doi.org/10.1016/S0091-679X(08)00409-3)
 106. Dubochet J. 2007. The physics of rapid cooling and its implications for cryoimmobilization of cells. *Methods Cell Biol* 79:7–21. [https://doi.org/10.1016/S0091-679X\(06\)79001-X](https://doi.org/10.1016/S0091-679X(06)79001-X)
 107. Marko M, Hsieh C, Schalek R, Frank J, Mannella C. 2007. Focused-ion-beam thinning of frozen-hydrated biological specimens for cryo-electron microscopy. *Nat Methods* 4:215–217. <https://doi.org/10.1038/nmeth1014>
 108. Vanhecke D, Studer L, Studer D. 2007. Cryoultramicrotomy, p 175–197. In Kuo J (ed), *Electron microscopy. methods in molecular biology*. Humana Press, Totowa, NJ.
 109. Al-Amoudi A, Norlen LPO, Dubochet J. 2004. Cryo-electron microscopy of vitreous sections of native biological cells and tissues. *J Struct Biol* 148:131–135. <https://doi.org/10.1016/j.jsb.2004.03.010>
 110. Dubochet J, Sartori Blanc N. 2001. The cell in absence of aggregation artifacts. *Micron* 32:91–99. [https://doi.org/10.1016/S0968-4328\(00\)00026-3](https://doi.org/10.1016/S0968-4328(00)00026-3)
 111. Zierold K. 1987. Cryoultramicrotomy, p 132–148. In Steinbrecht RA, Zierold K (ed), *Cryotechniques in biological electron microscopy*. Springer, Berlin.
 112. Han HM, Zuber B, Dubochet J. 2008. Compression and crevasses in vitreous sections under different cutting conditions. *J Microsc* 230:167–171. <https://doi.org/10.1111/j.1365-2818.2008.01972.x>
 113. Steinbrecht RA, Müller M. 1987. Freeze-substitution and freeze-drying, p 149–172. In Steinbrecht RA, Zierold K (ed), *Cryotechniques in biological electron microscopy*. Springer, Berlin.
 114. Zierold K, Zi K. 1986. The determination of wet weight concentrations of elements in freeze-dried cryosections from biological cells. *Scan Electron Microsc* 1986:713–724.
 115. Zierold K, Steinbrecht RA. 1987. Cryofixation of diffusible elements in cells and tissues for electron probe microanalysis, p 272–282. In Steinbrecht RA, Zierold K (ed), In *Cryotechniques in biological electron microscopy*. Springer, Berlin.
 116. Casanova G, Nolin F, Wortham L, Ploton D, Banchet V, Michel J. 2016. Shrinkage of freeze-dried cryosections of cells: investigations by EFTEM and cryo-CLEM. *Micron* 88:77–83. <https://doi.org/10.1016/j.micron.2016.06.005>
 117. Humbel B, Müller M. 1985. Freeze substitution and low temperature embedding. *Scan Electron Microsc* 4
 118. Ohno S. 2016. Freeze-substitution (FS) fixation method, p 199–202. In *In vivo cryotechnique in biomedical research and application for bioimaging of living animal organs*. Springer, Tokyo.
 119. Gavalis GS, Herranz M, Wakeman KC, Ripken C, Mitarai S, Gile GH, Keeling PJ, Leander BS. 2019. Dinoflagellate nucleus contains an extensive endomembrane network, the nuclear net. *Sci Rep* 9:839. <https://doi.org/10.1038/s41598-018-37065-w>
 120. Li J, Liu P, Menguy N, Zhang X, Wang J, Benzerara K, Feng L, Sun L, Zheng Y, Meng F, Gu L, Leroy E, Hao J, Chu X, Pan Y. 2022. Intracellular silicification by early-branching magnetotactic bacteria. *Sci Adv* 8:eabn6045. <https://doi.org/10.1126/sciadv.abn6045>

121. Girard-Dias W, Alcántara CL, Cunha-e-Silva N, Souza W, Miranda K. 2012. On the ultrastructural organization of *Trypanosoma cruzi* using cryopreparation methods and electron tomography. *Histochem Cell Biol* 138:821–831. <https://doi.org/10.1007/s00418-012-1002-8>
122. Gadelha APR, Cunha-e-Silva NL, de Souza W. 2013. Assembly of the *Leishmania amazonensis* flagellum during cell differentiation. *J Struct Biol* 184:280–292. <https://doi.org/10.1016/j.jsb.2013.09.006>
123. Lacomble S, Vaughan S, Gadelha C, Morphew MK, Shaw MK, McIntosh JR, Gull K. 2009. Three-dimensional cellular architecture of the flagellar pocket and associated cytoskeleton in trypanosomes revealed by electron microscope tomography. *J Cell Sci* 122:1081–1090. <https://doi.org/10.1242/jcs.045740>
124. Niyogi S, Jimenez V, Girard-Dias W, de Souza W, Miranda K, Docampo R. 2015. Rab32 is essential for maintaining functional acidocalcisomes, and for growth and infectivity of *Trypanosoma cruzi*. *J Cell Sci* 128:2363–2373. <https://doi.org/10.1242/jcs.169466>
125. Tomova C, Humbel BM, Geerts WJC, Entzeroth R, Holthuis JCM, Verkleij AJ. 2009. Membrane contact sites between apicoplast and ER in *Toxoplasma gondii* revealed by electron tomography. *Traffic* 10:1471–1480. <https://doi.org/10.1111/j.1600-0854.2009.00954.x>
126. Wendt C, Rachid R, de Souza W, Miranda K. 2016. Electron tomography characterization of hemoglobin uptake in *Plasmodium chabaudi* reveals a stage-dependent mechanism for food vacuole morphogenesis. *J Struct Biol* 194:171–179. <https://doi.org/10.1016/j.jsb.2016.02.014>
127. Augusto I, Girard-Dias W, Schoijet A, Alonso GD, Portugal RV, de Souza W, Jimenez V, Miranda K. 2024. Quantitative assessment of the nanoanatomy of the contractile vacuole complex in *Trypanosoma cruzi* Life Sci Alliance 7:e202402826. <https://doi.org/10.26508/lsa.202402826>
128. Miranda K, Girard-Dias W, Attias M, de Souza W, Ramos I. 2015. Three dimensional reconstruction by electron microscopy in the life sciences: an introduction for cell and tissue biologists. *Mol Reprod Dev* 82:530–547. <https://doi.org/10.1002/mrd.22455>
129. Peddie CJ, Genoud C, Kreshuk A, Meehan K, Micheva KD, Narayan K, Pape C, Parton RG, Schieber NL, Schwab Y, Titze B, Verkade P, Aubrey A, Collinson LM. 2022. Volume electron microscopy. *Nat Rev Methods Primers* 2:51. <https://doi.org/10.1038/s43586-022-00131-9>
130. Collinson LM, Bosch C, Bullen A, Burden JJ, Carzaniga R, Cheng C, Darrow MC, Fletcher G, Johnson E, Narayan K, Peddie CJ, Winn M, Wood C, Patwardhan A, Kleywegt GJ, Verkade P. 2023. Volume EM: a quiet revolution takes shape. *Nat Methods* 20:777–782. <https://doi.org/10.1038/s41592-023-01861-8>
131. Frank J. 2007. Introduction: principles of electron tomography, p 1–15. In *Electron tomography: methods for three-dimensional visualization of structures in the cell*. Springer, New York, NY.
132. Rohloff P, Montalvetti A, Docampo R. 2004. Acidocalcisomes and the contractile vacuole complex are involved in osmoregulation in *Trypanosoma cruzi*. *J Biol Chem* 279:52270–52281. <https://doi.org/10.1074/jbc.M410372200>
133. Aronova MA, Sousa AA, Leapman RD. 2011. EELS characterization of radiolytic products in frozen samples. *Micron* 42:252–256. <https://doi.org/10.1016/j.micron.2010.10.009>
134. Aronova MA, Leapman RD. 2012. Development of electron energy loss spectroscopy in the biological sciences. *MRS Bull* 37:53–62. <https://doi.org/10.1557/mrs.2011.329>
135. Aronova MA, Kim YC, Zhang G, Leapman RD. 2007. Quantification and thickness correction of EFTEM phosphorus maps. *Ultramicroscopy* 107:232–244. <https://doi.org/10.1016/j.ultramic.2006.07.009>
136. Bücking H, Beckmann S, Heyser W, Kottke I. 1998. Elemental contents in vacuolar granules of ectomycorrhizal fungi measured by EELS and EDXS: a comparison of different methods and preparation techniques. *Micron* 29:53–61. [https://doi.org/10.1016/S0968-4328\(97\)00059-0](https://doi.org/10.1016/S0968-4328(97)00059-0)
137. Vannier-Santos MA, Martiny A, Lins U, Urbina JA, Borges VM, de Souza W. 1999. Impairment of sterol biosynthesis leads to phosphorus and calcium accumulation in *Leishmania acidocalcisomes*. *Microbiology (Reading, Engl)* 145:3213–3220. <https://doi.org/10.1099/00221287-145-11-3213>
138. Bonhomme A, Pingret L, Bonhomme P, Michel J, Balossier G, Lhotel M, Pluot M, Pinon JM. 1993. Subcellular calcium localization in *Toxoplasma gondii* by electron microscopy and by X-ray and electron energy loss spectroscopies. *Microsc Res Tech* 25:276–285. <https://doi.org/10.1002/jemt.1070250403>
139. Soares Medeiros LC, Gomes F, Maciel LRM, Seabra SH, Docampo R, Moreno S, Plattner H, Hentschel J, Kawazoe U, Barrabin H, de Souza W, Damatta RA, Miranda K. 2011. Volutin granules of *Eimeria* parasites are acidic compartments and have physiological and structural characteristics similar to acidocalcisomes. *J Eukaryot Microbiol* 58:416–423. <https://doi.org/10.1111/j.1550-7408.2011.00565.x>
140. Moraes Moreira BL, Soares Medeiros LCA, Miranda K, de Souza W, Hentschel J, Plattner H, Barrabin H. 2005. Kinetics of pyrophosphate-driven proton uptake by acidocalcisomes of *Leptomonas wallacei*. *Biochem Biophys Res Commun* 334:1206–1213. <https://doi.org/10.1016/j.bbrc.2005.06.205>
141. Soares Medeiros LCA, Moreira BLM, Miranda K, de Souza W, Plattner H, Hentschel J, Barrabin H. 2005. A proton pumping pyrophosphatase in acidocalcisomes of *Herpetomonas* sp. *Mol Biochem Parasitol* 140:175–182. <https://doi.org/10.1016/j.molbiopara.2004.12.012>
142. Fernandez-Segura E, Warley A. 2008. Electron probe X-ray microanalysis for the study of cell physiology. *Methods Cell Biol* 88:19–43. [https://doi.org/10.1016/S0091-679X\(08\)00402-0](https://doi.org/10.1016/S0091-679X(08)00402-0)
143. Friel JJ, Lyman CE. 2006. Tutorial review: X-ray mapping in electron-beam instruments. *Microsc Microanal* 12:2–25. <https://doi.org/10.1017/S1431927606060211>
144. Ingram P, LeFurgey A, Roggly V, Shelburne J. 1999. Biomedical applications of microprobe analysis. Academic Press, San Diego.
145. Somlyo AP. 1984. Compositional mapping in biology: X rays and electrons. *J Ultrastruct Res* 88:135–142. [https://doi.org/10.1016/S0022-5320\(84\)80005-2](https://doi.org/10.1016/S0022-5320(84)80005-2)
146. Hall TA. 1979. Biological X-ray microanalysis. *J Microsc* 117:145–163. <https://doi.org/10.1111/j.1365-2818.1979.tb00236.x>
147. LeFurgey A, Ingram P, Blum JJ. 1990. Elemental composition of polyphosphate-containing vacuoles and cytoplasm of *Leishmania major*. *Mol Biochem Parasitol* 40:77–86. [https://doi.org/10.1016/0166-6851\(90\)90081-v](https://doi.org/10.1016/0166-6851(90)90081-v)
148. Ramos IB, Miranda K, Ulrich P, Ingram P, LeFurgey A, Machado EA, de Souza W, Docampo R. 2010. Calcium- and polyphosphate-containing acidocalcisomes in chicken egg yolk. *Biol Cell* 102:421–434. <https://doi.org/10.1042/BC20100011>
149. Zaluzec NJ. 2019. Improving the sensitivity of X-ray microanalysis in the analytical electron microscope. *Ultramicroscopy* 203:163–169. <https://doi.org/10.1016/j.ultramic.2018.11.008>
150. Schlossmacher P, Klenov DO, Freitag B, von Harrach HS. 2010. Enhanced detection sensitivity with a new windowless XEDS system for AEM based on silicon drift detector technology. *Microsc Today* 18:14–20. <https://doi.org/10.1017/S1551929510000404>
151. Zaluzec NJ. 2023. X-ray spectrometry in the era of Aberration-corrected electron optical beam lines. *Microsc Microanal* 29:334–340. <https://doi.org/10.1017/S143192762200068X>
152. Williams DB, Carter CB. 2009. *Transmission electron microscopy second*. Springer.
153. McMullan G, Faruqi AR, Clare D, Henderson R. 2014. Comparison of optimal performance at 300keV of three direct electron detectors for use in low dose electron microscopy. *Ultramicroscopy* 147:156–163. <https://doi.org/10.1016/j.ultramic.2014.08.002>
154. Thompson RF, Walker M, Siebert CA, Muench SP, Ranson NA. 2016. An introduction to sample preparation and imaging by cryo-electron microscopy for structural biology. *Methods* 100:3–15. <https://doi.org/10.1016/j.jmeth.2016.02.017>
155. Egerton RF. 2009. Electron energy-loss spectroscopy in the TEM. *Rep Prog Phys* 72:016502. <https://doi.org/10.1088/0034-4885/72/1/016502>
156. Schröder RR, Hofmann W, Ménétret JF. 1990. Zero-loss energy filtering as improved imaging mode in cryoelectronmicroscopy of frozen-hydrated specimens. *J Struct Biol* 105:28–34. [https://doi.org/10.1016/1047-8477\(90\)90095-T](https://doi.org/10.1016/1047-8477(90)90095-T)
157. Fukuda Y, Laugks U, Lučić V, Baumeister W, Danev R. 2015. Electron cryotomography of vitrified cells with a Volta phase plate. *J Struct Biol* 190:143–154. <https://doi.org/10.1016/j.jsb.2015.03.004>
158. Danev R, Buijsse B, Khoshouei M, Plitzko JM, Baumeister W. 2014. Volta potential phase plate for in-focus phase contrast transmission electron microscopy. *Proc Natl Acad Sci USA* 111:15635–15640. <https://doi.org/10.1073/pnas.1418377111>
159. Axelrod JJ, Zhang JT, Petrov PN, Glaeser RM, Müller H. 2024. Modern approaches to improving phase contrast electron microscopy. *Curr Opin Struct Biol* 86:102805. <https://doi.org/10.1016/j.sbi.2024.102805>
160. Schaffer M, Pfeffer S, Mahamid J, Kleindiek S, Laugks T, Albert S, Engel BD, Rummel A, Smith AJ, Baumeister W, Plitzko JM. 2019. A cryo-FIB lift-out technique enables molecular-resolution cryo-ET within native *Caenorhabditis elegans* tissue. *Nat Methods* 16:757–762. <https://doi.org/10.1038/s41592-019-0497-5>

161. Schiötz OH, Kaiser CJO, Klumpe S, Morado DR, Poege M, Schneider J, Beck F, Klebl DP, Thompson C, Plitzko JM. 2024. Serial lift-out: sampling the molecular anatomy of whole organisms. *Nat Methods* 21:1684–1692. <https://doi.org/10.1038/s41592-023-02113-5>
162. Tuijtel MW, Cruz-León S, Kreysing JP, Welsch S, Hummer G, Beck M, Turoňová B. 2024. Thinner is not always better: optimizing cryo-lamellae for subtomogram averaging. *Sci Adv* 10:eadk6285. <https://doi.org/10.1126/sciadv.adk6285>
163. Klein S, Wimmer BH, Winter SL, Kolovou A, Laketa V, Chlanda P. 2021. Post-correlation on-lamella cryo-CLEM reveals the membrane architecture of lamellar bodies. *Commun Biol* 4:1–12. <https://doi.org/10.1038/s42003-020-01567-z>
164. Kuba J, Mitchels J, Hovorka M, Erdmann P, Berka L, Kirmse R, König J, De Bock J, Goetze B, Rigort A. 2021. Advanced cryo - tomography workflow developments – correlative microscopy, milling automation and cryo - lift - out. *J Microsc* 281:112–124. <https://doi.org/10.1111/jmi.12939>
165. Klein S, Wachsmuth-Melm M, Winter SL, Kolovou A, Chlanda P. 2021. Cryo-correlative light and electron microscopy workflow for cryo-focused ion beam milled adherent cells. *Methods Cell Biol* 162:273–302. <https://doi.org/10.1016/bs.mcb.2020.12.009>
166. Pierson JA, Yang JE, Wright ER. 2024. Recent advances in correlative cryo-light and electron microscopy. *Curr Opin Struct Biol* 89:102934. <https://doi.org/10.1016/j.sbi.2024.102934>
167. Goodenough U, Heiss AA, Roth R, Rusch J, Lee J-H. 2019. Acidocalcisomes: ultrastructure, biogenesis, and distribution in microbial eukaryotes. *Protist* 170:287–313. <https://doi.org/10.1016/j.protis.2019.05.001>
168. Ramakrishnan S, Asady B, Docampo R. 2018. Acidocalcisome-mitochondrion membrane contact sites in *Trypanosoma brucei*. *Pathogens* 7:33. <https://doi.org/10.3390/pathogens7020033>
169. Xiong ZH, Ridgley EL, Enis D, Olness F, Ruben L. 1997. Selective transfer of calcium from an acidic compartment to the mitochondrion of *Trypanosoma brucei*. Measurements with targeted aequorins. *J Biol Chem* 272:31022–31028. <https://doi.org/10.1074/jbc.272.49.31022>
170. Boonrungsiman S, Gentleman E, Carzaniga R, Evans ND, McComb DW, Porter AE, Stevens MM. 2012. The role of intracellular calcium phosphate in osteoblast-mediated bone apatite formation. *Proc Natl Acad Sci USA* 109:14170–14175. <https://doi.org/10.1073/pnas.1208916109>
171. Hosein ID. 2021. The promise of calcium batteries: open perspectives and fair comparisons. *ACS Energy Lett* 6:1560–1565. <https://doi.org/10.1021/acsenergylett.1c00593>